Improving the Sanding Process of Black Spruce Wood for Surface Quality and Water-Based Coating Adhesion

Julie Cool
Roger E. Hernández

Abstract

The sanding of black spruce wood prior to coating application was optimized for feed speed and grit size. As feed speed increased, the surface roughness and the surface energy of the samples increased. For the different sanding programs, reductions of the surface roughness and the contact angles were observed with a finer grit abrasive. The initial pull-off strength was statistically similar regardless of the feed speed and grit size. However, both the feed speed and the grit size affected coating adhesion following the accelerated weathering treatment. Because there was no correlation between the surface quality parameters and the pull-off strength, the latter had to be measured to determine coating performance on black spruce wood. In the present work, a two-stage sanding program combined with a feed speed of 17 m/min resulted in good surface quality and pull-off strength.

Sanding is one of the most skill-based, time-consuming, and expensive operations in the wood industry (Taylor et al. 1999) as well as being hazardous to health (d'Errico et al. 2009). Because sanding produces defect-free uniform surfaces (Richter et al. 1995), it is widely used in the industry prior to the application of coating or glue. However, although sanding is often associated with wood planing with negative rake angles (Stewart 1980, 1989; Heurtematte et al. 1985; Juan 1992), the cutting forces involved are generally higher than those observed in planing (Stewart 1980, 1989; Hall and Heard 1982; Stewart and Crist 1982). According to several authors, this produces an important layer of damaged and crushed cells (Jokerst and Stewart 1976; Stewart and Crist 1982; Murmanis et al. 1983, 1986; Caster et al. 1985; de Moura and Hernández 2005, 2006b). Furthermore, sanded samples are characterized by lumens clogged by fine dust, scratches, and packets of microfibrils torn out from cell walls (Murmanis et al. 1983, 1986; de Moura and Hernández 2006b). Crushing and clogging of cells hinder penetration of liquid coatings on sanded surfaces (de Meijer et al. 1998), while light fibrillation and scratches accelerate their spread. The benefits of fibrillation for mechanical adhesion of coating films have been shown for sanded surfaces of sugar maple wood (de Moura and Hernández 2005). When working with low-density wood species such as softwoods, higher material removal rates and surface roughness are expected (Sinn et al. 2004, Saloni et al. 2005).

Black spruce (*Picea mariana* (Mill.) Britton, Sterns & Poggenb.) is one of the most important boreal tree species in Canada. Its properties and abundance make it a valuable resource, and its wood is widely used in the pulp and paper industry and in construction applications such as lumber and glued structural members. However, little information is available on its sanding behavior. This species has only been included in general studies on Canadian woods undertaken by Lihra and Ganev (1999). The authors used a single-stage P120-grit aluminum oxide sanding program. Black spruce wood showed a similar behavior to that of other spruce-pine-fir species and only yielded 52 percent of defect-free surfaces. However, Cool and Hernández (2011) recently reported that sanding with a single-stage P80-grit aluminum oxide sanding program induced good mechanical adhesion because of an important level of fibrillation and the presence of micro-ruptures that increased the actual surface available for

The authors are, respectively, PhD candidate and Professor, Centre de recherche sur le bois, Département des sciences du bois et de la forêt, Univ. Laval, Québec, Canada (julie.cool.1@ulaval.ca, roger.hernandez@sbf.ulaval.ca [corresponding author]). This paper was received for publication in March 2011. Article no. 11-00032.

Forest Prod. J. 61(5):372–380.

mechanical anchorage of poly (vinyl acetate) glue. Therefore, optimizing machining parameters could further improve surface quality and adhesion. This could favor the use of black spruce wood for appearance purposes. Hence, the purpose of this work was to evaluate the effects of three feed speeds and three grit sandpapers on the surface anatomy, roughness, and wetting properties as well as on the adhesion of a water-based coating on black spruce specimens.

Materials and Methods

Testing materials

Black spruce wood was selected for this study. Two hundred seventy 860-mm (longitudinal [L]) flat sawn boards were kiln dried and stored in a conditioning room at 20°C and 40 percent relative humidity (RH) until they reached 10 percent equilibrium moisture content (EMC). After conditioning, all sections were machined at 52-mm (tangential [T]) width and 22-mm (radial [R]) thickness. The average (455 kg/m^3) and standard deviation (35 kg/m^3) of basic density (ovendry mass divided by green volume) were measured by crosscutting a 25-mm-long section from each specimen. The specimens were then divided into nine groups having an average density of 455 kg/m^3 each. Subsequently, each group underwent a surfacing treatment. After surfacing, samples were resectioned to prepare specimens for roughness (50 mm [L]), microscopy (25.4 mm [L]), wettability (160 mm [L]), and coating application (620 mm [L]). After coating, two matched samples were sawn. One of the samples underwent an accelerated aging treatment before being submitted to the adhesion test. The second sample was kept unaged.

Machining treatments

The sanding treatment was performed with a Costa wide-belt sander equipped with silicon carbide close-coat paper-backed sanding belts. Three sanding programs were tested: 100-grit, 100-150-grit, and 100-120-180-grit stages. The 100-grit, 120-grit, 150-grit, and 180-grit sanding belts worked at a removal depth of 0.3, 0.2, 0.1, and 0.1 mm, respectively. All sanding belts were installed onto a drum, and feeding was carried out fiberwise. Three feed speeds were used: 4, 10.5, and 17 m/min. Oscillating blowers performed cooling and cleaning of the belt during sanding.

Microscopic evaluation

Ten-millimeter cubes were used to observe tangential and end-grain surfaces. Tangential surfaces served mainly to evaluate the level of fibrillation and open lumens. End-grain surfaces were used to evaluate the level of cell damage and coating penetration. One of the end-grain surfaces in the sample was carefully prepared with a razor blade mounted on a microtome. All cubes were then desiccated with phosphorous pentoxide (P_2O_5) for a week and mounted on standard aluminum stubs with silver paint. Environmental scanning electron microscopy (ESEM) micrographs were taken for two representative machined samples for each machining treatment.

Surface topography measurements

Roughness measurements were carried out on defect-free zones with a Micromeasure confocal microscope equipped with a 3-mm optical pen fixed at 27 mm from the surface. The precision of this pen was 0.4 μm. A surface of 12.5 mm (L) by 12.5 mm (T) was analyzed per sample at 20°C. The data were collected with the Surface Map 2.4.13 software using an acquisition frequency of 300 Hz and a scanning speed of 12.5 mm/s. The three-dimensional roughness parameters were determined by using the Mountain software. A cut-off length of 2.5 mm combined with a Robust Gaussian filter (International Organization for Standardization [ISO] 16610-31; ISO 2002) were used for calculations. The arithmetical mean deviation of the profile (S_A), the maximum profile peak height (S_P), and the maximum profile valley depth (S_V) were calculated according to ISO 4287 (ISO 1998). The reduced peak height (S_{PK}) and the reduced valley depth (S_{VK}) were calculated from the Abbot curve according to ISO 13565-2 (ISO 1996).

Wettability measurements

Wetting properties were evaluated within 12 hours following the machining treatments. Wetting analyses were performed with an FTÅ D200 imaging goniometer at 20°C. Small droplets (~6 μL) of pure water were added to the sanded wood surfaces with an injection microsyringe. A frame grabber recorded the changes in droplet profile during the first 120 seconds of wetting. The measurements were carried out in the longitudinal direction since wetting is more important fiberwise. Contact angle was calculated as a mean of both sides of the drop in order to compensate for any horizontal variations. The wetting rate was calculated as the variation of the contact angle ($\Delta\theta$) over the first 30 seconds of wetting (Δt) to assess the spreading and penetration of pure water. For surface energy measurements, the initial contact angle of formamide was also measured. The nonpolar and polar components of the surface energy were calculated using the harmonic mean approach (Wu 1971).

Coating applications procedure

The machined surfaces were coated within 8 hours after the machining treatments. During this period, samples were placed face against face in order to keep contamination at minimum levels. An acrylic water-based coating, Laurentide-Innocryl PF, was air sprayed (150 μm) at room temperature according to the manufacturer's specifications. The coating was then cured in an infrared oven following a methodology established with the coating manufacturer.

Accelerated aging

Half of the specimens underwent an accelerated aging treatment in a Cincinnati SubZero environmental stimulation chamber (WM-906-MP2H-3-SC/WC) having temperature and RH precisions of ±1°C and ±3 percent, respectively. The treatment was based on American Society for Testing and Materials (ASTM) D3459 (ASTM 1998) and consisted of four cycles of 48 hours at 50°C and 10 percent RH followed by 48 hours at 50°C and 90 percent RH. Prior to the treatment, the ends of the specimens were sealed with paraffin to reduce the moisture exchange through the cross section. After aging, the specimens were conditioned at 20°C and 40 percent RH until they reached their initial EMC (10%).

Adhesion tests

Adhesion of the accelerated aged films as well as those unaged was evaluated by means of a pull-off test according to ASTM D4541 (ASTM 2002). An MTS QT5 universal testing machine having a maximal capacity of 5 kN and ±0.12 percent precision was used. Small 20-mm-diameter dollies were glued on the film surface with Araldite 2011 two-part epoxy resin. After 24 hours of curing at 20°C and 40 percent RH, the perimeters of the glued dollies were carefully incised to prevent propagation of failures out of the tested area. Pulling was applied at 1 mm/min until separation of the dolly from the substrate. The maximum normal pull strength at rupture was recorded.

Statistical analyses

A factorial design with two factors, feed speed and grit size, was established for the experiment. The data followed a randomized block design and results from the mechanical tests were analyzed with the mixed procedure in SAS as repeated measures. Surface topography, wettability, and surface energy were analyzed as a 1-way analysis of variance, following the generalized linear model procedure. Mean difference comparison tests were performed at 5 percent probability level when required. Simple correlations between surface quality parameters and pull-off results were studied using the correlation procedure. The analysis was done in SAS statistical package, version 9.2 (SAS 2007).

Results and Discussion

Microscopy

Sanding treatments induced a certain level of damage in the black spruce wood surfaces. For all studied conditions, the earlywood cells were more damaged than those of latewood. Subsurface damage was reduced when a finer grit size was used, but little difference was visible among the three feed speeds. The waterborne coating did not penetrate into the cells; it only filled the lumens that were available at the surface through tearing of cell walls. Such damage mainly occurred in earlywood since the cell walls were thinner than those of latewood layers.

The single-stage sanding program, using P100-grit abrasive sandpaper, crushed and deformed earlywood cells down to a depth of about 100 μm (Fig. 1A). The subsurface damage did not consist of a uniform layer of crushed or deformed cells, in such a way that some earlywood cells appeared sound. Sanding is comparable to an orthogonal planing process having a negative rake angle (Stewart 1980, 1989; Heurtematte et al. 1985; Juan 1992). As a result, the negative normal cutting force is important, and Type III chips are most likely to be produced. This could contribute to the crushing of earlywood cells since their stiffness is lower than that of latewood cells. More specifically, some latewood cells were deformed and slightly crushed while most remained sound (Fig. 1B). Their thicker cell walls, in comparison with those of the earlywood, offer a greater stiffness and strength to the cutting action. However, microruptures were induced in the middle lamella of latewood cells and extended down the first two to three cells (~50 μm). As mentioned previously by Cool and Hernández (2011), these microruptures could act as discontinuities during the moisturizing–drying cycles of the weathering. Thus, the microruptures could help in releasing stresses produced in wood by weathering.

When a second step with a finer grit paper (P150 grit) was added, the level of subsurface damage in the samples was reduced (Fig. 2). Cells of earlywood were crushed and

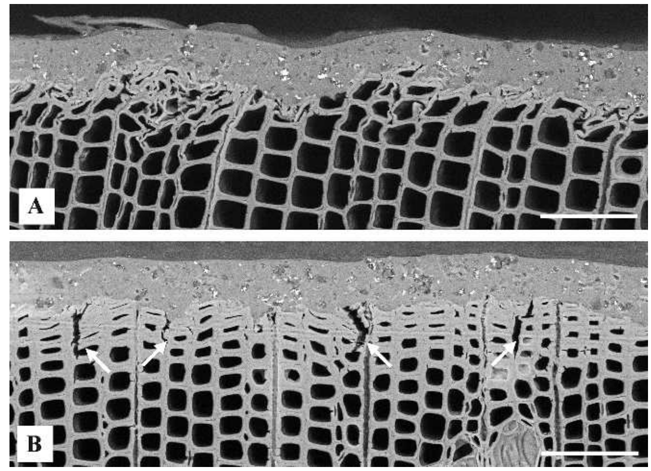

Figure 1.—Transverse environmental scanning electron microscopy micrographs of black spruce wood samples that were sanded with P100-grit abrasive sandpaper at 10.5 m/min (A) and 17 m/min (B). Arrows show microruptures induced in latewood of sanded samples. Scale bars = 100 μm.

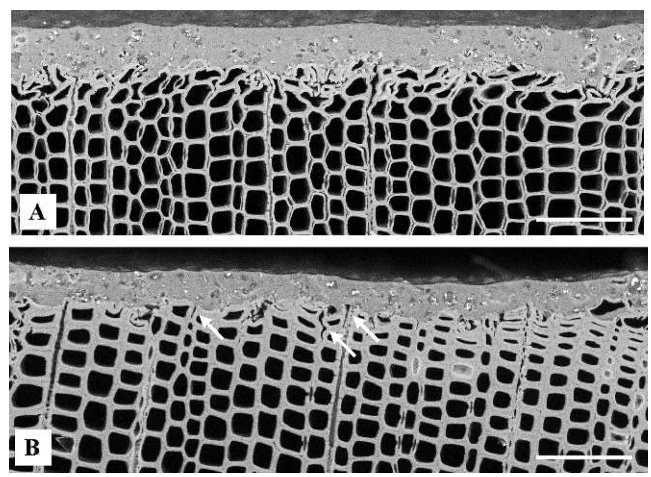

Figure 2.—Transverse environmental scanning electron microscopy micrographs of black spruce wood samples that were sanded with a two-stage sanding program (P100-P150 grit) at 4 m/min (A) and 10.5 m/min (B). Arrows show microruptures induced in latewood of sanded samples. Scale bars = 100 μm.

deformed down the first two to three cells (~50 μm). The addition of the P150-grit stage eliminated the topmost layers of cells that were most damaged, leaving lower subsurface damage. In latewood, microruptures were generated in the middle lamella and extended down ~20 μm into the samples. The cell wall deformation was reduced compared with the P100-grit sanding program.

The three-stage sanding program created surfaces that suffered little deformation during the process (Fig. 3). As mentioned previously, each step of the program eliminated the topmost layers of damaged cells. This further reduced the cell damage observed. In earlywood, only the first two to three cells (~50 μm) were lightly deformed and crushed during machining. In latewood, microruptures that extended down ~20 μm were present as was light cell-wall deformation.

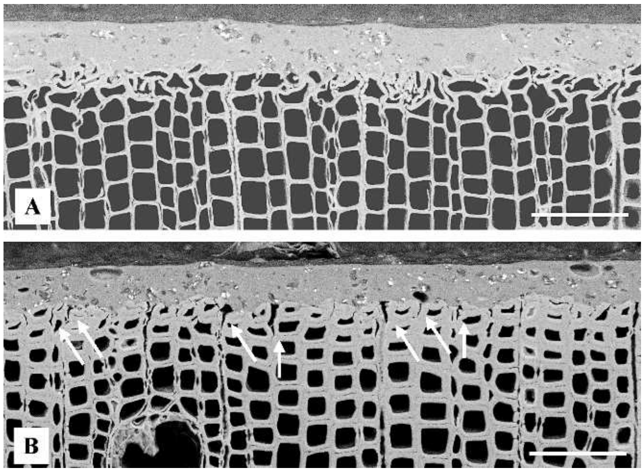

Figure 3.—Transverse environmental scanning electron microscopy micrographs of black spruce wood samples that were sanded with a three-stage sanding program (P100-P120-P180 grit) at 17 m/min (A) and 10.5 m/min (B). Arrows show microruptures induced in latewood of sanded samples. Scale bars = 100 μm.

Surface topography

All sanded surfaces were characterized by a certain fibrillation (Figs. 4 through 6). The abrasives also produced grooves in the surfaces that were visible at the microscopic level and should favor the spread of coating in the longitudinal direction. As expected, the width and depth of the grooves as well as the level of fibrillation were reduced when using finer grit sizes. Hence, coarser grits could increase the spread of coating, although the presence of dust in these grooves could slow the process. Clusters of microfibrils as well as partially torn cell walls and crushed tracheids were visible on the surfaces. If not firmly attached to the surface, this fibrillation could reduce coating adhesion. On the other hand, adhesion could be increased by the level of fibrillation because it increases the actual surface available for mechanical anchorage of the coating. As the material removal rate increases with feed speed (Saloni et al. 2005), sanded surfaces of sugar maple wood were characterized by more damage (de Moura and Hernández 2006a). This should also have been the case in black spruce, but no visible differences were observed on the micrographs (Figs. 4 through 6). Even though each additional step minimized the irregularities and defects produced by the previous sandpaper (Carrano et al. 2002, de Moura and Hernández 2006a, Ratnasingam and Scholz 2006), the surface was similarly affected during the two- and three-stage sanding programs (Figs. 5 and 6). Compared with samples sanded with the single-stage program, the extent of the damage was reduced. The level of fibrillation was lower and the grooves were thinner (Figs. 4 through 6).

Macroscopically, no major surface defects were observed on the samples. All the surface roughness parameters were significantly affected by the interaction between the feed speed and grit size (Table 1). As reported previously, surface roughness increased with the feed speed (Carrano et al. 2002, de Moura and Hernández 2006a) and the coarseness of the abrasive (Carrano et al. 2002, Sinn et al. 2004, de Moura and Hernández 2006a, Ratnasingam and Scholz 2006). The grit size affected all roughness

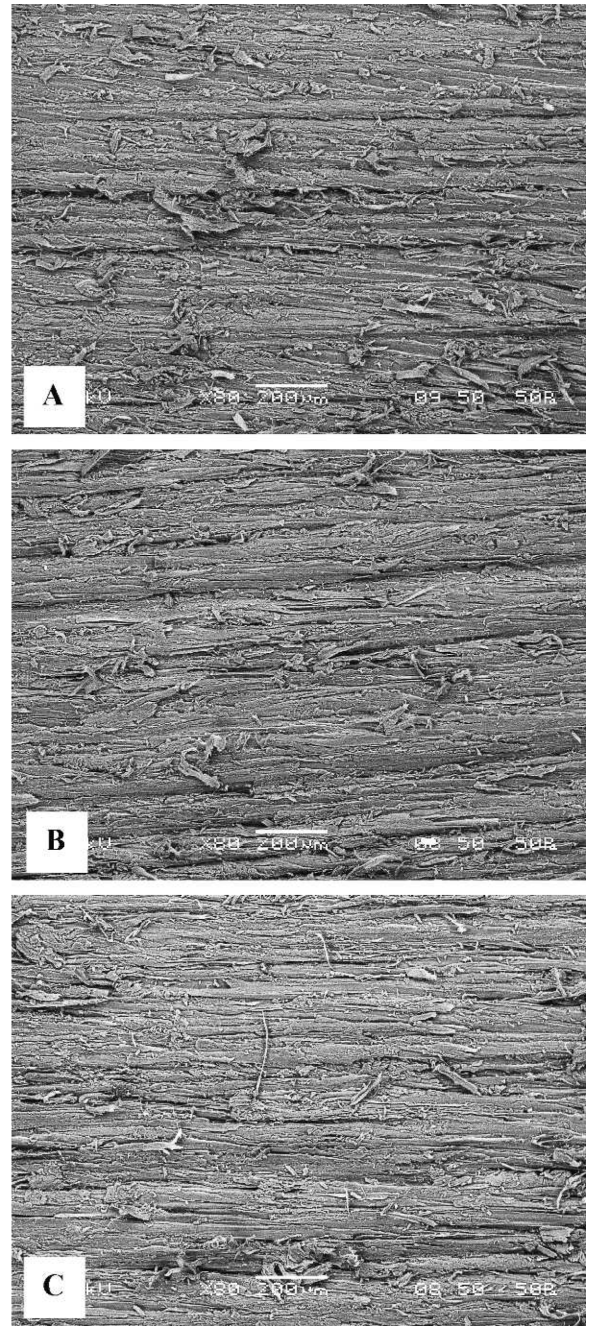

Figure 4.—Tangential environmental scanning electron microscopy micrographs of black spruce wood samples that were sanded with a single-stage sanding program (P100 grit) at 4 m/min (A), 10.5 m/min (B), and 17 m/min (C).

parameters more than did feed speed (Table 1). The significant interaction indicates that the effect of grit size was more important for 10.5 m/min feed speed than for the other two feed speeds.

The mean surface roughness parameter (S_A) was significantly smaller when the lower feed speed was used regardless of the sanding program (Table 1). More specifically, the samples were significantly smoother when a feed speed of 4 or 10.5 m/min was combined with the three-stage sanding program (P100-P150-P180 grit). The lower level of fibrillation as well as the thinner grooves left

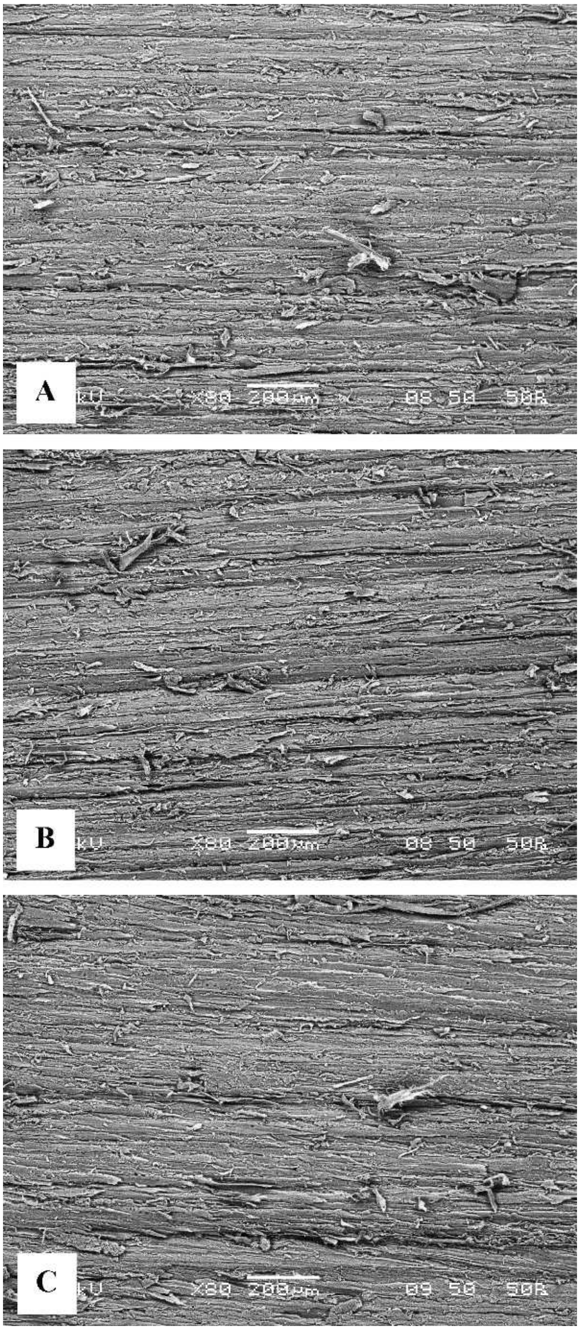

Figure 5.—Tangential environmental scanning electron microscopy micrographs of black spruce wood samples that were sanded with a two-stage sanding program (P100-P150 grit) at 4 m/min (A), 10.5 m/min (B), and 17 m/min (C).

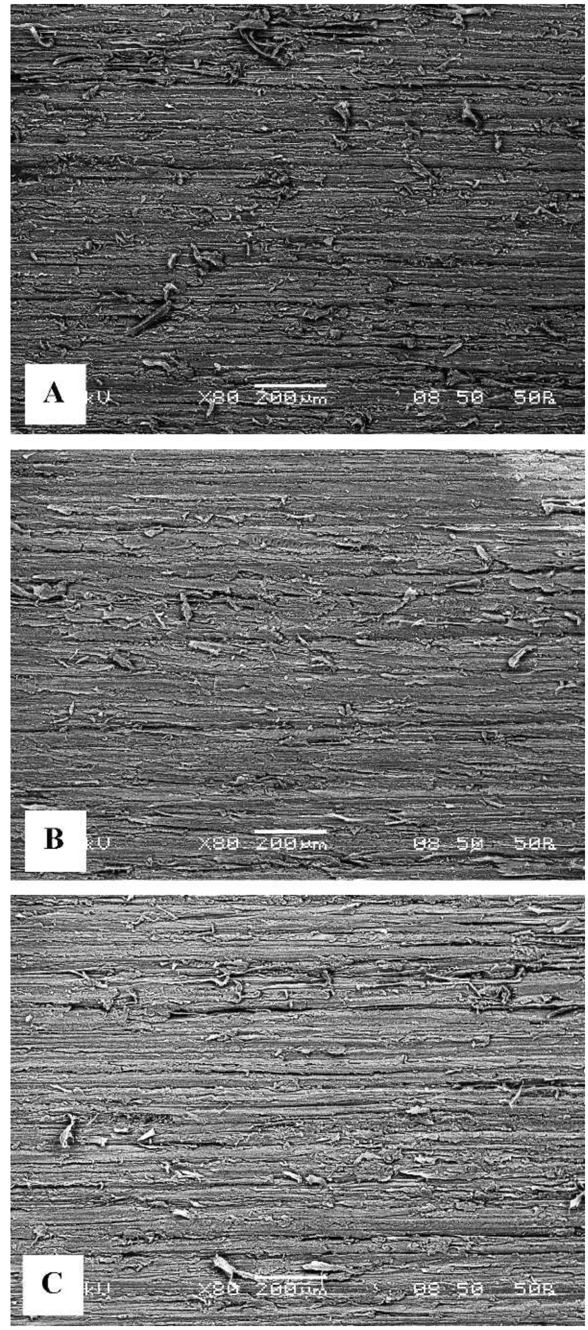

Figure 6.—Tangential environmental scanning electron microscopy micrographs of black spruce wood samples that were sanded with a three-stage sanding program (P100-P120-P180 grit) at 4 m/min (A), 10.5 m/min (B), and 17 m/min (C).

on these surfaces contributed to the decrease in S_A. These surfaces were also more uniform, which decreased surface roughness. In addition, the parameters S_P and S_V, associated with the maximum profile peak height and the maximum profile valley depth, respectively, were almost equivalent for all sanding conditions. This confirms that the sanding process uniformly affected black spruce wood surfaces. Similar results were obtained by Cool and Hernández (2011) when sanding the same species. The lowest values of S_P and S_V were obtained for a feed speed of 4 m/min combined with the two-stage (P100-P150-grit) and three-stage (P100-P150-P180-grit) sanding treatments as well as for the 10.5 m/min feed speed combined with the three-stage sanding program. In summary, low feed speeds and fine grit sandpapers created uniform black spruce surfaces.

The parameter S_{PK}, associated with the level of fuzzy grain (Fujiwara et al. 2005, Gurau et al. 2005), was low for samples sanded with a feed speed of 4 m/min combined with the two- and three-stage sanding treatments as well as for the 10.5 m/min feed speed combined with the three-stage sanding program. Since this defect was not observed on the samples, the parameter S_{PK} could be associated with the

Table 1.—Three-dimensional surface roughness parameters (μm) of black spruce wood specimens prepared by sanding at three different feed speeds and grit sizes.[a]

Feed speed (m/min)	Grit size	S_A	S_P	S_V	S_{PK}	S_{VK}
4	P100	6.1 (0.1) A	27.5 (0.8) A	31.6 (0.8) A	6.3 (0.2) A	9.5 (0.3) A
	P100-P150	3.6 (0.1) B	17.8 (0.6) B	19.9 (0.7) BC	4.0 (0.2) BC	5.5 (0.2) B
	P100-P120-P180	3.3 (0.1) C	16.3 (0.5) B	18.6 (0.7) B	3.8 (0.1) B	5.3 (0.2) BD
10.5	P100	6.8 (0.1) D	30.8 (1.1) C	34.4 (0.8) D	7.4 (0.3) D	10.0 (0.3) A
	P100-P150	4.1 (0.1) E	21.2 (0.6) D	24.4 (0.5) E	4.5 (0.1) E	6.2 (0.2) C
	P100-P120-P180	3.3 (0.1) C	16.8 (0.5) B	18.8 (0.7) B	3.8 (0,1) B	4.9 (0.2) D
17	P100	6.5 (0.1) F	32.2 (1.0) C	36.5 (0.9) F	6.8 (0.2) D	10.0 (0.2) A
	P100-P150	4.2 (0.1) E	24.0 (0.8) E	25.3 (0.8) E	4.9 (0.2) F	6.5 (0.2) C
	P100-P120-P180	3.6 (0.0) B	20.5 (0.7) D	21.4 (0.6) C	4.1 (0.1) C	5.3 (0.1) BD

[a] Values are the means (standard errors of the means) of 30 replicates. Means within a column followed by the same letter are not significantly different at the 5 percent probability level. S_A = arithmetical mean deviation of the profile; S_P = maximum profile peak height; S_V = maximum profile valley depth; S_{PK} = reduced peak height; S_{VK} = reduced valley depth.

level of fibrillation. In that respect, Table 1 shows that the level of fibrillation was reduced as feed speed and grit of sandpaper decreased. This is also visible on the ESEM micrographs (Figs. 4 through 6).

The parameter S_{VK} has been associated with the anatomical features of wood such as the number of open lumens (Fujiwara et al. 2005). According to Figures 4 through 6, the natural anatomical features were not visible on the tangential surfaces. S_{VK} would instead be related to the number and dimensions of grooves left on the surfaces by the abrasive. As mentioned previously, the first stage of the sanding process generates larger and deeper grooves and the subsequent steps decrease the importance of those grooves. This is in agreement with results obtained for S_{VK} (Table 1). As shown in Figures 4 through 6, the three-stage sanding program generated surfaces with the thinnest grooves and the single-stage program (P100 grit) produced samples with the largest grooves.

Wettability

Spreading and penetration of pure water was more important for samples prepared by the single-stage program (P100 grit; Fig. 7). As mentioned previously, these samples exhibited the highest roughness because of the larger and deeper grooves than those produced by finer sandpapers. Many authors have reported that increasing surface roughness accelerates liquid spreading (Wenzel 1936, Parker and Taylor 1966, Lewis and Forrestal 1969, Moredo et al. 1996, Aydin et al. 2006, de Moura and Hernández 2006b).

To quantify the spreading and penetration, the progression of the contact angle of pure water was measured and the parameter $\Delta\theta/\Delta t$ was calculated as the difference in contact angle within the first 30 seconds of wetting. Feed speed had a significant impact on the initial contact angle, while grit size affected the contact angle measured subsequently. In the case of $\Delta\theta/\Delta t$, both the feed speed and grit size had a significant effect on this parameter. As shown in Figure 7 and Tables 1 and 2, the single-stage sanding program generated surfaces having the best wetting properties because of their higher surface roughness. The two- and three-stage sanding programs created surfaces with similar features. Although the grooves were more numerous, water spreading and penetration decreased because of their

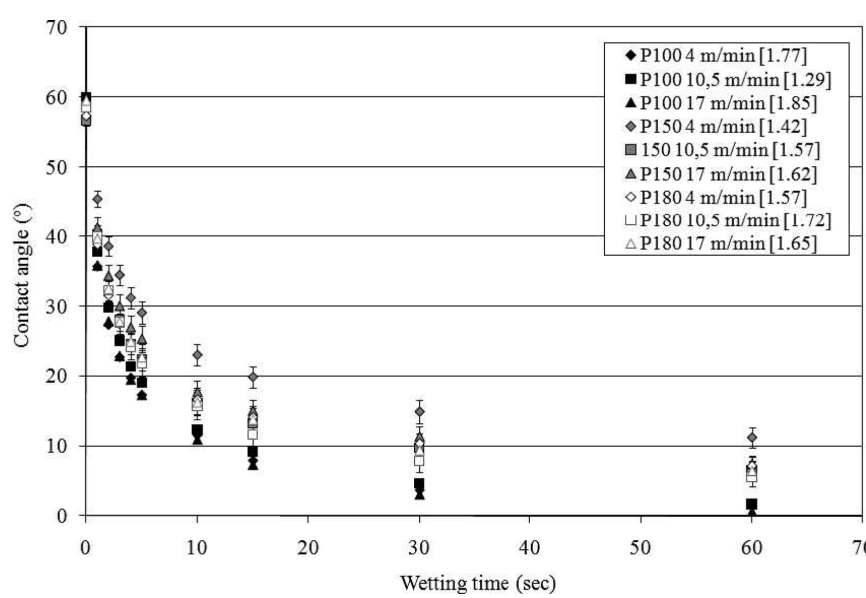

Figure 7.—Progression of the contact angle of pure water on black spruce wood samples sanded with three different grit sizes and three feed speeds. For every sanding condition, the mean value of the wetting rate is in brackets.

Table 2.—Wetting rate and surface energy determined by the two-liquid harmonic mean method.[a]

Feed speed (m/min)	Grit size	Δθ/Δ*t* (°/s)	Surface energy (mJ/m^2)		
			Nonpolar	Polar	Total
4	P100	1.8 (0.0) ADF	14.2 (0.5) D	32.0 (0.9) AB	46.2 (0.6) A
	P100-P150	1.4 (0.1) B	15.4 (0.4) C	30.3 (0.6) BC	45.7 (0.4) A
	P100-P120-P180	1.6 (0.1) C	16.0 (0.5) BC	29,8 (0.7) BCD	45.8 (0.4) A
10.5	P100	1.8 (0.0) A	16.6 (0.4) B	27.7 (0.6) E	44.2 (0.4) AB
	P100-P150	1.6 (0.0) C	13.7 (0.5) D	32.4 (0.8) A	46.2 (0.5) AB
	P100-P120-P180	1.7 (0.0) DE	18.1 (0.6) A	27.6 (0.9) E	45.7 (0.5) AB
17	P100	1.9 (0.0) AF	13.7 (0.4) D	31.1 (0.7) AB	44.8 (0.5) B
	P100-P150	1.6 (0.0) CE	16.8 (0.5) AB	27.7 (0.9) DE	44.5 (0.6) B
	P100-P120-P180	1.7 (0.1) CDEF	16.4 (0.5) BC	28.3 (1.0) CDE	44.6 (0.7) B

[a] Values are the means (standard errors of the means) of 30 replicates. Means within a column followed by the same letter are not significantly different at the 5 percent probability level.

reduced width and depth. These results are also in agreement with the calculated surface energy components.

The surface energy components obtained in this study (Table 2) are similar to those obtained by de Meijer et al. (2000) for latewood of spruce wood calculated by the geometric mean approach. The nonpolar or disperse component of the surface energy, related to the reversible hydrogen links, was significantly affected by the feed speed and grit size. Smaller values were obtained for the single-stage program (P100 grit), while higher values were calculated for the two-stage program (P100-P150 grit) at 17 m/min and for the three-stage program (P100-P120-P180 grit) at 10.5 m/min. Compared with the single-stage program, more heat could be generated during the multistage sanding programs, which may inactivate the wood surfaces. When a second and/or third stage was added to the process, it prolonged the contact between the abrasives and the wood, which would contribute to further increasing surface inactivation. Although cutting tool temperature could reach up to 400°C during machining (Sheikh-Ahmad et al. 2003), wood surface temperature only increased 30°C in 90°-0° orthogonal cutting and peeling of panels (Okumura et al. 1993, Sheikh-Ahmad and McKenzie 1997). The fact that the cutting tool and surface temperature increase with cutting forces (Sheikh-Ahmad and McKenzie 1997, Sheikh-Ahmad et al. 2003) suggests that the temperature increase will vary with the machining process. Since sanding has proved to generate more important cutting forces than those observed in peripheral planing (Stewart 1980, 1989; Hall and Heard 1982; Stewart and Crist 1982), the surface temperature increase during sanding could be more important than 30°C. As a result, a multistage sanding program in which the surface is modified repetitively could lead to a higher degree of inactivation than a single-stage program. This is reflected by an enhancement in the nonpolar component of the surface energy (Table 2) and a reduction in the spread and penetration of pure water on the sanded surfaces (Fig. 7). The same conclusions can be drawn from the results of the polar component because higher values are associated with more hydrophilic surfaces (Gindl et al. 2004). However, results must be interpreted with caution because there was little difference among the treatments.

Adhesion tests

Results of the pull-off tests are summarized in Table 3. Before aging, all sanding treatments yielded statistically similar pull-off strength. A similar behavior was reported with sanded paper birch wood coated with two types of finishing products (Hernández and Cool 2008).

After the accelerated aging treatment, the pull-off strength was reduced by about 30 percent (Table 3). The water-based coating adhesion was significantly affected by both the feed speed and the grit size. The interaction between the feed speed and grit size was not statistically significant. Thus, mean comparisons were performed separately for each source of variation by pooling the values of the other source of variation (Table 4). Samples sanded at 4 m/min feed speed yielded a higher pull-off strength, although not significantly different from those sanded at 17 m/min. Table 4 also shows that coating adhesion after aging was more important on samples surfaced by the three-stage sanding program. This treatment was statistically similar to the two-stage sanding program. There was no correlation between the pull-off strength and the surface quality parameters (roughness and wettability) that were evaluated.

No significant differences were detected among the treatments with regard to the percentage of loss in adhesion during the weathering treatment (Table 3). However, the loss in adhesion seemed to be lower at 4 m/min feed speed compared with the other feed speeds (25%, compared with 28% and 31% for 10.5 and 17 m/min, respectively, all sanded programs pooled). The loss in adhesion also appeared to be reduced by the addition of finer sandpapers (31%, 29%, and 25% for the single-, two-, and three-stage programs, respectively, all feed speeds pooled). Thus, a

Table 3.—Pull-off strength, before and after an accelerated aging treatment, and loss in adhesion of a waterborne coating applied on black spruce wood specimens prepared by sanding at three different feed speeds and grit sizes.[a]

Feed speed (m/min)	Grit size	Before aging (MPa)	After aging (MPa)	Loss in adhesion (%)
4	P100	4.4 (0.1)	3.3 (0.2)	27
	P100-P150	4.6 (0.1)	3.2 (0.1)	29
	P100-P120-P180	4.3 (0.1)	3.5 (0.1)	20
10.5	P100	4.4 (0.2)	3.1 (0.1)	29
	P100-P150	4.1 (0.1)	3.0 (0.1)	28
	P100-P120-P180	4.3 (0.2)	3.1 (0.1)	28
17	P100	4.5 (0.2)	2.8 (0.1)	38
	P100-P150	4.7 (0.1)	3.3 (0.1)	29
	P100-P120-P180	4.6 (0.2)	3.3 (0.1)	27

[a] Values are the means (standard errors of the means) of 30 replicates.

Table 4.—Results of the mean difference comparison tests performed on the data of pull-off strength after an accelerated aging treatment of a waterborne coating applied on black spruce wood specimens prepared by sanding.

	After aging (MPa)[a]
Feed speed (m/min)[b]	
4	3.32 (0.08) A
10.5	3.07 (0.07) B
17	3.14 (0.08) AB
Grit size[c]	
P100	3.04 (0.08) B
P100-P150	3.17 (0.08) AB
P100-P120-P180	3.31 (0.07) A

[a] Values are the means (standard errors of the means) of 90 replicates. Means followed by the same letter are not significantly different at the 5 percent probability level.
[b] Grit size pooled.
[c] Feed speed pooled.

surface characterized by lower subsurface damage and fibrillation could favor the adhesion of the studied waterborne coating on sanded black spruce wood. Surfaces produced by the three-stage sanding program at 4 m/min feed speed exhibited adequate fibrillation to enhance mechanical anchorage. Furthermore, the lower subsurface damage prevented the degradation of the wood-coating interphase (Table 3). These surfaces were also defined by lower surface roughness and wetting properties. Therefore, the mechanical adhesion was more important than the chemical one during adherence of the studied coating on black spruce.

According to the results (Tables 3 and 4), a feed speed of 4 m/min induced similar pull-off strength to that of 17 m/min and the three-stage program was similar to the two-stage program. Hence, the two-stage program at a feed speed of 17 m/min should be more appropriate because it induces surfaces characterized by good quality and pull-off strength. More specifically, this high feed speed would increase production rates. Paper costs would also be reduced compared with the three-stage program. As mentioned previously, no correlations were obtained between the surface quality parameters and the pull-off strength. As a consequence, the pull-off strength has to be performed in order to measure coating performance on black spruce wood.

Conclusions

Feed speed and grit size of sandpapers had an impact during sanding on the surface anatomy and consequently on the roughness and wetting properties. Coarser grit size and higher feed speeds contributed to increased surface roughness and improved wetting properties. Samples prepared with coarser grit sandpaper (single-stage program) underwent a greater reduction in pull-off strength during the accelerated weathering treatment because they had subsurface damage. The two-stage sanding program appeared better as it resulted in pull-off strength values similar to those generated by the three-stage sanding program. Production costs could therefore be decreased. A feed speed of 17 m/min is recommended because it did not impair the adhesion of coating and would increase production rates. Since the surface quality parameters were not correlated with pull-off strength, it would be interesting, in future research, to work with other factors. For instance, multiple regression techniques could be used to predict the pull-off strength. Significant surface quality parameters could be combined in order to develop a global factor that would be correlated with pull-off strength. Working with other softwoods and finishing products could also help to understand why no correlations were obtained.

Acknowledgments

The authors thank Luc Germain, Daniel Bourgault, Benoit Harbour, and Dany Bourque for valuable assistance, as well as Renaud Gilbert from Société Laurentide. This research was supported by the ForValueNet, a Natural Sciences and Engineering Research Council of Canada strategic network on forest management for value-added products.

Literature Cited

American Society for Testing and Materials (ASTM). 1998. Standard test method for humid-dry cycling for coatings on wood and wood products. ASTM D3459. ASTM, Philadelphia, Pennsylvania.

American Society for Testing and Materials (ASTM). 2002. Standard test method for pull-off strength of coatings using portable adhesion testers. ASTM D4541. ASTM, Philadelphia, Pennsylvania.

Aydin, I., G. Colakoglu, and S. Hiziroglu. 2006. Surface characteristics of spruce veneers and shear strength of plywood as a function of log temperature in peeling process. *Int. J. Solids Struct*. 43(20): 6140–6147.

Carrano, A. L., J. B. Taylor, and R. Lemaster. 2002. Parametric characterization of peripheral sanding. *Forest Prod. J*. 52(9):44–50.

Caster, D., N. Kutscha, and G. Leick. 1985. Gluability of sanded lumber. *Forest Prod. J*. 35(4):45–52.

Cool, J. and R. E. Hernández. 2011. Evaluation of four surfacing methods on black spruce wood in relation to poly (vinyl acetate) gluing performance. *Wood Fiber Sci*. 43(2):194–205.

de Meijer, M., S. Haemers, W. Cobben, and H. Militz. 2000. Surface energy determination of wood: Comparison of methods and wood species. *Langmuir* 16(24):9352–9359.

de Meijer, M., K. Thurich, and H. Militz. 1998. Comparative study on penetration characteristics of modern wood coatings. *Wood Sci. Technol*. 32(5):347–365.

de Moura, L. F. and R. E. Hernández. 2005. Evaluation of varnish coating performance for two surfacing methods on sugar maple wood. *Wood Fiber Sci*. 37(2):355–366.

de Moura, L. F. and R. E. Hernández. 2006a. Effects of abrasive mineral, grit size and feed speed on the quality of sanded surfaces of sugar maple wood. *Wood Sci Technol*. 40(6):517–530.

de Moura, L. F. and R. E. Hernández. 2006b. Evaluation of varnish coating performance for three surfacing methods on sugar maple wood. *Forest Prod. J*. 56(11/12):130–136.

d'Errico, A., S. Pasian, A. Baratti, R. Zanelli, S. Alfonzo, L. Gilardi, F. Beatrice, A. Bena, and G. Costa. 2009. A case-control study on occupational risk factors for sino-nasal cancer. *Occup. Environ. Med*. 66(7):448–455.

Fujiwara, Y., Y. Fujii, and S. Okumura. 2005. Relationship between roughness parameters based on material ratio curve and tactile roughness for sanded surfaces of two hardwoods. *J. Wood Sci*. 51(3):274–277.

Gindl, M., A. Reiterer, G. Sinn, and S. E. Stanzl-Tschegg. 2004. Effects of surface ageing on wettability, surface chemistry, and adhesion of wood. *Holz Roh- Werkst*. 63(4):273–280.

Gurau, L., H. Mansfield-Williams, and M. Irle. 2005. Processing roughness of sanded wood surfaces. *Holz Roh- Werkst*. 63(1):43–52.

Hall, A. and J. Heard. 1982. Wood Finishing and Refinishing. Holt, Rinehart and Winston, New York. 196 pp.

Hernández, R. E. and J. Cool. 2008. Evaluation of three surfacing methods on paper birch wood in relation to water- and solvent-borne coating performance. *Wood Fiber Sci*. 40(3):459–469.

Heurtematte, J., M. Orus, P. Pouzeau, and R. Le Sage. 1985. Usinage du bois: à l'usage des élèves des enseignements technologiques, des

professionnels de l'industrie intéressée par la formation permanente. Delagrave, Paris. 127 pp.
International Organization for Standardization (ISO). 1996. Geometrical product specifications (GPS). Surface texture. Profile method; Surfaces having stratified functional properties. Part 2: Height characterisation using the linear material ratio curve. ISO 13565-2. ISO, London.
International Organization for Standardization (ISO). 1998. Geometrical product specifications (GPS). Surface texture. Profile method. Terms. Definitions and surface texture parameters. ISO 4287. ISO, London.
International Organization for Standardization (ISO). 2002. Geometrical product specifications (GPS)—Filtration part 31: Robust profile filters. Gaussian regression filters. ISO 16610-31. ISO, London.
Jokerst, R. W. and H. A. Stewart. 1976. Knife- versus abrasive-planed wood: Quality of adhesive bonds. *Wood Fiber* 8(2):107–113.
Juan, J. 1992. Comment bien usiner le bois. Centre Technique du Bois et de l'Ameublement, Paris. 140 pp.
Lewis, A. F. and L. J. Forrestal. 1969. Adhesion of coatings. *In:* Treatise on Coatings. Vol. 2. Characterization of Coatings: Physical Techniques. R. R. Myers and J. S. Long (Eds.). Marcel Dekker, New York. pp. 57–98.
Lihra, T. and S. Ganev. 1999. Machining properties of eastern species and composite panels. Forintek Canada Corporation, Division de l'Est, Ste-Foy, Québec. 62 pp.
Moredo, C. C., T. Sakuno, and T. Kawada. 1996. The improvement of bond strength properties and surface characteristics of resinous woods. *J. Adhes*. 59(1–4):183–195.
Murmanis, L., B. H. River, and H. A. Stewart. 1983. Microscopy of abrasive-planed and knife-planed surfaces in wood-adhesive bonds. *Wood Fiber Sci*. 15(2):102–115.
Murmanis, L., B. H. River, and H. A. Stewart. 1986. Surface and subsurface characteristics related to abrasive-planing conditions. *Wood Fiber Sci*. 18(1):107–117.
Okumura, S., S. Nanba, and M. Noguchi. 1993. Thermographic temperature measurement of tool-chip-work system in slow-speed wood cutting. *In:* Proceedings of the 11th International Wood Machining Seminar, May 25–27, 1993, Oslo; Norwegian Institute of Wood Technology, Oslo. pp. 41–55.
Parker, R. S. R. and P. Taylor. 1966. Adhesion and Adhesives. Pergamon Press, Oxford. 142 pp.
Ratnasingam, J. and F. Scholz. 2006. Optimal surface roughness for high-quality finish on rubberwood (*Hevea brasiliensis*). *Holz Roh-Werkst*. 64(4):343–345.
Richter, K., W. C. Feist, and M. T. Knaebe. 1995. The effect of surface roughness on the performance of finishes. Part 1. Roughness characterization and stain performance. *Forest Prod. J*. 45(7/8):91–97.
Saloni, D. E., R. L. Lemaster, and S. D. Jackson. 2005. Abrasive machining process characterisation on material removal rate, final surface texture, and power consumption for wood. *Forest Prod. J*. 55(12):35–41.
SAS. 2007. SAS/STAT users' guide, version 9.2. SAS Institute Inc., Cary, North Carolina.
Sheikh-Ahmad, J. Y., C. M. Lewandowski, J. A. Bailey, and J. S. Stewart. 2003. Experimental and numerical method for determining temperature distribution in a wood cutting tool. *Exp. Heat Transfer* 16(4):255–271.
Sheikh-Ahmad, J. Y. and W. M. McKenzie. 1997. Measurement of tool wear and dulling in the machining of particleboard. *In:* Proceedings of the 13th International Wood Machining Seminar, June 17–20, 1997, Vancouver, British Columbia; University of British Columbia and Forintek Canada Corporation, Vancouver. pp. 659–670.
Sinn, G., M. Gindl, A. Reiterer, and S. Stanzl-Tschegg. 2004. Changes in the surface properties of wood due to sanding. *Holzforschung* 58(3): 246–251.
Stewart, H. A. 1980. Some surfacing defects and problems related to wood moisture content. *Wood Fiber* 12(3):175–182.
Stewart, H. A. 1989. Fixed-knife pressure-bar planing method reduces or eliminates subsurface damage. *Forest Prod. J*. 39(7/8):66–70.
Stewart, H. A. and J. B. Crist. 1982. SEM examination of subsurface damage of wood after abrasive and knife planing. *Wood Sci*. 14(3): 106–109.
Taylor, J. B., A. L. Carrano, and R. L. Lemaster. 1999. Quantification of process parameters in a wood sanding operation. *Forest Prod. J*. 49(5): 41–46.
Wenzel, R. N. 1936. Resistance of solid surfaces to wetting by water. *Ind. Eng. Chem*. 28(8):988–994.
Wu, S. 1971. Calculation of interfacial tension in polymer systems. *J. Polym. Sci. Part C* 34:19–30.